

Supplementary Information

Entropy-Driven DNA Timer Fluorescence Sensor for One-pot

Sequential Detection of Three Respiratory Viruses

Chiliang Lin^a, Shaoyun Peng^a, Junling He^a, Yong Tang^a, Haimin Zou^b, and Chen Zhou^{a*}

^a West China School of Public Health and West China Fourth Hospital, Sichuan University, Chengdu, 610041, China

^b Department of Clinical Laboratory, Sichuan Clinical Research Center for Cancer, Sichuan Cancer Hospital & Institute, Sichuan Cancer Center, Affiliated Cancer Hospital of University of Electronic Science and Technology of China, Chengdu, 610041, China

Table of Contents

Table S1 Sequences of the ssDNA oligonucleotides used in entropy-driven DNA timer fluorescence sensor	3
Table S2 Comparison of the sensitivity of the proposed fluorescence sensor with other methods for detection of SARS-CoV-2, RSV, and Flu A.....	4
Table S3 Sequences of the DNA oligonucleotides used in specificity assessments.....	4
Table S4 RT-PCR results for clinical samples.....	5
Fig. S1 Structural simulations of substrate probes in (a) traditional EDC and (b) gap EDC using NUPACK.....	6
Fig. S2 Electrophoretic validation of (a) gap EDC system and (b) traditional EDC system	6
Fig. S3 Stability assessment of DNA timer biosensor	7
Fig. S4 Time-dependent fluorescence intensity profiles for detection of three viruses in 12 clinical samples and positive quality control of SARS-CoV-2 (S), RSV (R), and Flu A (F)	8
Text S1 Optimization and Characterization of the EDC systems.	9
Fig. S5 Secondary structure predictions of molecular beacon strands generated by NUPACK software.....	9
Fig. S6 Polyacrylamide gel electrophoresis (PAGE) analysis of strand MB opening mediated by strand SB.....	9
Fig. S7 Fluorescence analysis of strand MB interaction with strand SB and potential interference from strand F	10
References	10

Table S1 Sequences of the ssDNA used in entropy-driven DNA timer fluorescence sensor

Name	Sequence (5'-3')
S-C	GCAGCAGTACGCACACAATC
S-OP	ATTCAATTCTAGGCACTTTCTCCATCC
S-SB	TAGATTTAATGTGCCCGCAGCAGTACGCA
S-S	GATTGTGTGCGTACTGCTGCGGGCGTGGATGGAGAAAGTGCCTA
S-F	TAGGCACTTTCTCCATCCACGCCCCGCAGCAGTACGCA
S-MB	HEX-CCGCCAGCGGGCACATTAATCTTGCGGG-Dabeyl
F-C	GCCCAGTGAGCGAGGACTGCA
F-SB	TGAGCGAGGACTGCACTGGTATAATTAGCTA
F-OP	GGCTGCTGACATGACCTGATCTATATGA
F-S	CAGGTCATGTCAGCAGCCTACCAGTGCAGTCCTCGCTCACTGGGCTCACTATTC
F-F	TGAGCGAGGACTGCACTGGTAGGCTGCTGACATGACCTG
F-MB	6-FAM-CGGCCTAATTATACCAGTGGCGCCG-Dabeyl
F-Br	GAATAGT(8-oxo-dG)AGCCCAG
R-C	GAGGTAGCTCCAGAATACAGG
R-SB	GATTAATAATAGACGAGGTAGCTCCAGA
R-OP	TAAGCGATGGCAGGTAGTGAGAGGATCG
R-S	CTCTCTTATCCTGTATTCTGGAGCTACCTCGTCATCGATCCTCTCACTACCTG
R-F	CAGGTAGTGAGAGGATCGATGACGAGGTAGCTCCAGA
R-MB	ATTO 425-CGCCGTACCTCGTCTATTTAATCGGCG- Dabeyl
R-Br	A(2'-deoxyuridine)ACAGG(2'-deoxyuridine)AAG(2'-deoxyuridine)AG(2'-deoxyuridine)G

Table S2 Comparison of the sensitivity of the proposed fluorescence sensor with other methods for detection of SARS-CoV-2, RSV, and Flu A

Virus	Strategies	Analytical time	LOD	Ref.
SARS-CoV-2	Electrochemical RT-LAMP	30 min	2.5 pg/mL	1
SARS-CoV-2	CHA-ELISA	2 h	1 nM	2
SARS-CoV, Flu A, and RSV	RT-PCR-SPR	2 h	2 nM	3
SARS-CoV-2	LSPR	15 min	0.22 pM	4
Flu A	Microfluidic array LAMP	60 min	2 pg/mL	5
Flu A & RSV	CHA-LFIA	30 min	5 pM	6
SARS-CoV-2, IVA, IVB, and RSV	RT-LAMP	30 min	35 copies/ μ L	7
SARS-CoV-2, Flu A, and RSV	DNA timer	45 min	4.8 pM	This work
SARS-CoV-2, Flu A, and RSV	RT-PCR	2 h	500 copies/mL	(Sansure Biotech Inc.)

Notes: RT-LAMP, reverse-transcriptase loop-mediated isothermal amplification; CHA, catalytic hairpin assembly; ELISA, enzyme-linked immunosorbent assay; RT-PCR, reverse transcription-polymerase chain reaction; SPR, surface plasmon resonance; LSPR, localized surface plasmon resonance; LFIA, lateral flow immunoassay.

Table S3 Sequences of the DNA oligonucleotides used in specificity assessments

Name	Sequence (5'-3')
F-L1	GCCGAGTGAGCGAGGACTGCA
F-L2.1	GCCCAGTGAGCCAGGACTGCA
F-L2.2	GC GG GAGTGAGCGAGGACTGCA
S-L1	GCAGCAGTACGCACAGAATC
S-L2.1	GCAGCA C TACGCACACAATC
S-L2.2	GCAGCAGTACGCAGAGAATC
R-L1	GAGGTAGCTCCAGAATAGAGG
R-L2.1	GAGGTAGCTGCAGAATACAGG
R-L2.2	GAGGTAGCTCCAGAATAG AC G

Notes: mismatched bases were highlighted in red

Table S4 RT-PCR results¹ for clinical samples (*n*=3)

Clinical Samples	Ct value		
	SARS-CoV-2	RSV	Flu A
1	UD	UD	35.72
2	UD	UD	37.28
3	UD	35.89	UD
4	UD	UD	UD
5	UD	UD	UD
6	36.24	UD	UD
7	UD	UD	UD
8	UD	35.37	UD
9	UD	UD	UD
10	UD	UD	UD
11	UD	UD	UD
12	35.30	UD	UD
P-QC	32.85	33.02	36.61

Notes: UD, undetermined; P-QC: positive quality control.

¹: The RT-PCR assay was conducted using a commercially available kit (Sansure Biotech Inc), following the manufacturer's instructions strictly.

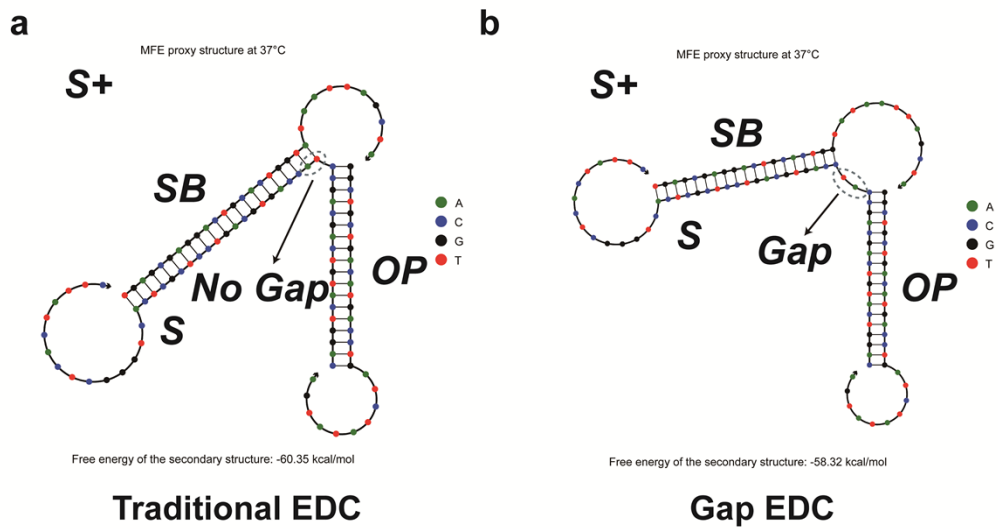


Fig. S1 Structural simulations of substrate probes in (a) traditional EDC and (b) gap EDC using NUPACK.

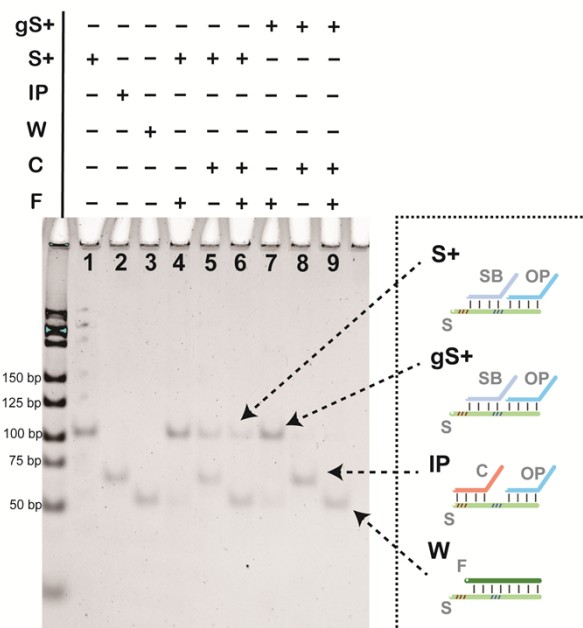


Fig. S2 Electrophoretic validation of traditional EDC system (lane 4~6) and gap EDC system (lane 7~9). +: added; -: not added. gS+: S+ of gap EDC. All experiments were performed in triplicate.

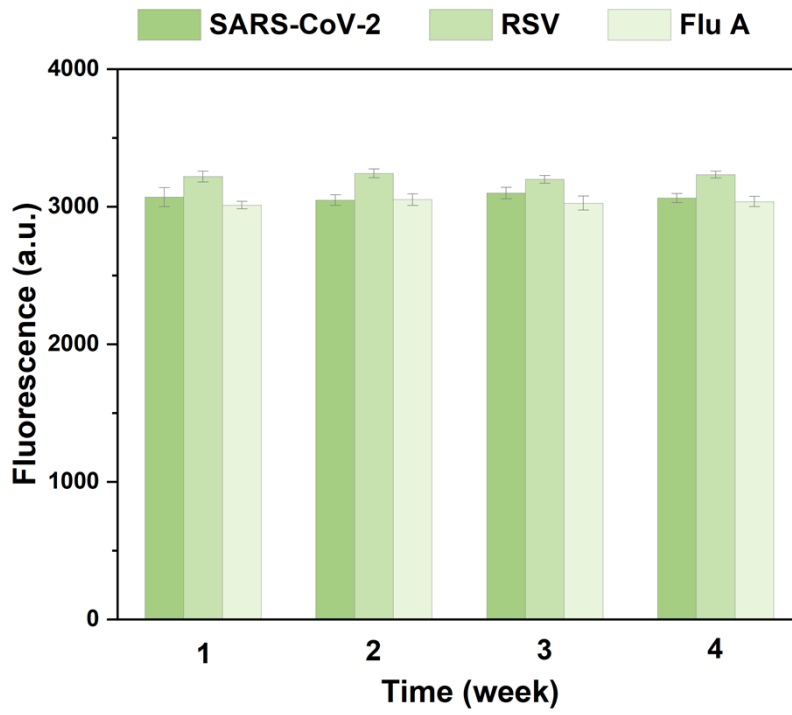


Fig. S3 Stability assessment of DNA timer biosensor: fluorescence signals were quantified weekly over four weeks. All experiments were performed in triplicate, and error bars represented standard deviations.

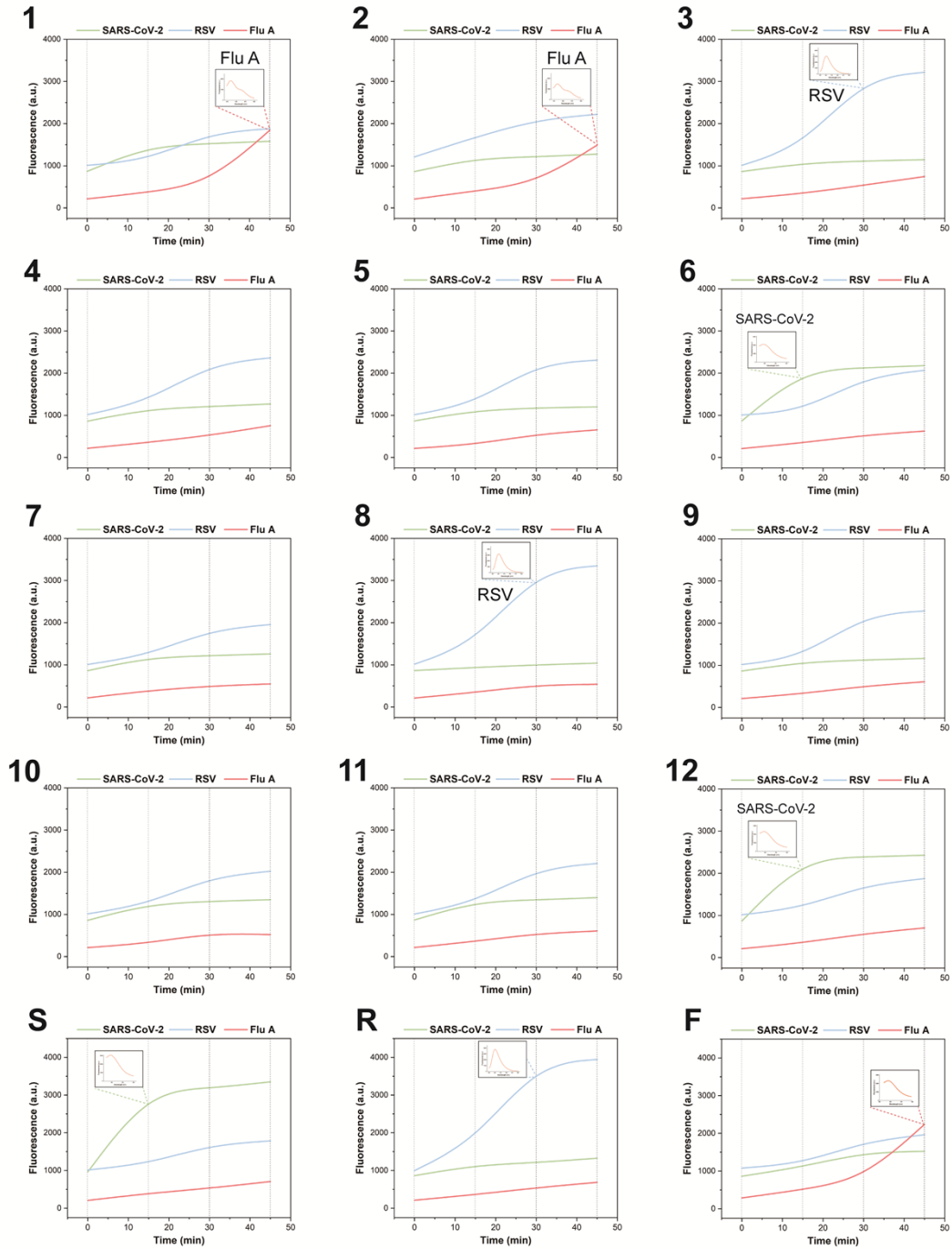


Fig. S4 Time-dependent fluorescence intensity profiles for detection of three viruses in 12 clinical samples and positive quality control of SARS-CoV-2 (S), RSV (R), and Flu A (F). Positive samples are identified by characteristic fluorescence signatures at virus-specific time points. All experiments were performed in triplicate.

Text S1 Optimization and Characterization of the EDC systems

The molecular beacons (strand MB) were well designed to serve as the signal transduction component of the systems. Computational analysis using NUPACK confirmed the formation of a stable hairpin structure, which effectively minimized background fluorescence signals (Fig. S5). Experimental validation demonstrated that the fluorescence emission from strand MB occurred exclusively in the presence of target molecules, confirming the system's specificity and robustness (Fig. S6). Furthermore, control experiments established that strand MB maintained its structural integrity and signal generation capability without interference from other system components, consistently producing strong, target-dependent fluorescence signals (Fig. S7).

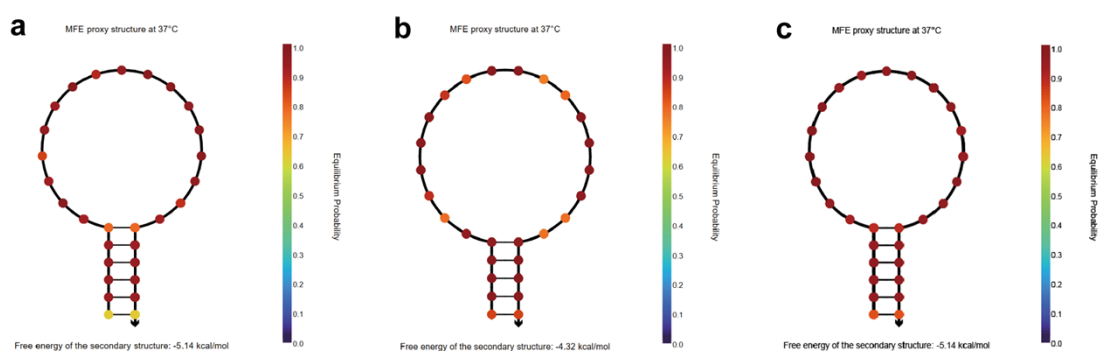


Fig. S5 Secondary structure predictions of molecular beacon strands generated by NUPACK software: (a) S-MB, (b) R-MB, and (c) F-MB.

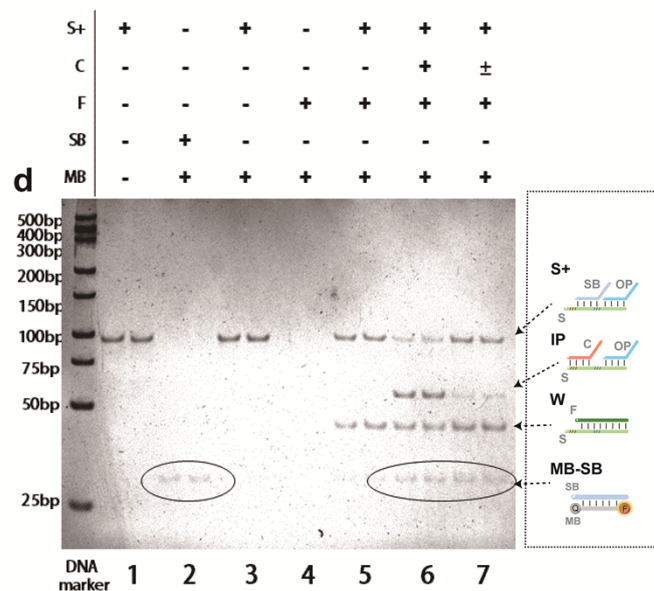


Fig. S6 Polyacrylamide gel electrophoresis (PAGE) analysis of strand MB opening mediated by strand SB. (+): added; (±): not added. All experiments were performed in triplicate.

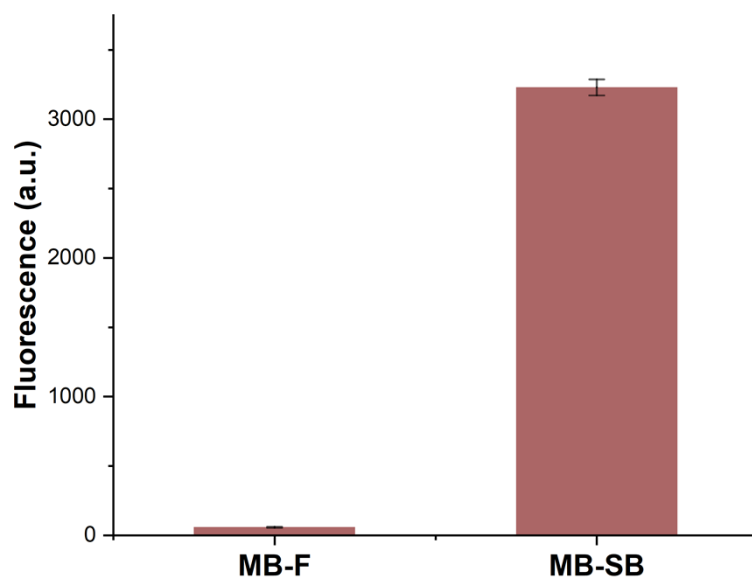


Fig. S7 Fluorescence analysis of strand MB interaction with strand SB and potential interference from strand F. All experiments were performed in triplicate, and error bars represented standard deviations.

References

1. R. G. Ramírez-Chavarría, E. Castillo-Villanueva, B. E. Alvarez-Serna, J. Carrillo-Reyes, R. M. Ramírez-Zamora, G. Buitrón and L. Alvarez-Icaza, *J Environ Chem Eng*, 2022, **10**, 107488.
2. J. Y. Do, J. Y. Jeong and C. A. Hong, *Talanta*, 2021, **233**, 122505.
3. L. Shi, Q. Sun, J. a. He, H. Xu, C. Liu, C. Zhao, Y. Xu, C. Wu, J. Xiang, D. Gu, J. Long and H. Lan, *Bio-Medical Materials and Engineering*, 2015, **26**, S2207-S2216.
4. G. Qiu, Z. Gai, Y. Tao, J. Schmitt, G. A. Kullak-Ublick and J. Wang, *ACS Nano*, 2020, **14**, 5268-5277.
5. R. Wang, R. Zhao, Y. Li, W. Kong, X. Guo, Y. Yang, F. Wu, W. Liu, H. Song and R. Hao, *Lab on a Chip*, 2018, **18**, 3507-3515.
6. H. Wu, M. Zou, X. Fan, F. Su, F. Xiao, M. Zhou, Y. Sun, F. Zhao and G. Wu, *ACS Omega*, 2022, **7**, 15074-15081.
7. J. Lim, K. Koprowski, R. Stavins, N. Xuan, T.-H. Hoang, J. Baek, V. Kindratenko, L. Khaertdinova, A. Y. Kim, M. Do, W. P. King, E. Valera and R. Bashir, *ACS Sensors*, 2024, **9**, 4058-4068.